Original Article

Application of low-dose FDG-PET/MRI for quantification of lung changes in pediatric patients with cystic fibrosis: a new inflammatory index

Ricarda Schwarz[1], Jürgen Frank Schäfer[1], Philipp Utz[2], Ute Graepler-Mainka[2], Helmut Dittmann[3], Mareen Sarah Kraus[4], Michael Esser[1]^

[1]Department of Diagnostic and Interventional Radiology, University Hospital Tübingen, Tübingen, Germany; [2]Department of General Pediatrics, Hematology and Oncology, Children's Hospital, University Hospital Tübingen, Tübingen, Germany; [3]Department of Nuclear Medicine and Clinical Molecular Imaging, University Hospital Tübingen, Tübingen, Germany; [4]Department of Diagnostic Radiology, Dalhousie University, IWK Health Centre, Halifax, NS, Canada

Contributions: (I) Conception and design: R Schwarz, JF Schäfer, P Utz, M Esser; (II) Administrative support: JF Schäfer, U Graepler-Mainka, M Esser; (III) Provision of study materials or patients: JF Schäfer, P Utz, H Dittmann, MS Kraus; (IV) Collection and assembly of data: R Schwarz, U Graepler-Mainka, H Dittmann, MS Kraus; (V) Data analysis and interpretation: R Schwarz, P Utz, H Dittmann, M Esser; (VI) Manuscript writing: All authors; (VII) Final approval of manuscript: All authors.

Correspondence to: Michael Esser, MD. Department of Diagnostic and Interventional Radiology, University Hospital Tübingen, Hoppe-Seyler-Straße 3, 72076 Tübingen, Germany. Email: Michael.Esser@med.uni-tuebingen.de.

Background: Clinical severity and progression of lung disease in cystic fibrosis (CF) are significantly influenced by the degree of lung inflammation. Non-invasive quantitative diagnostic tools are desirable to differentiate structural and inflammatory lung changes in order to help prevent chronic airway disease. This might also be helpful for the evaluation of longitudinal effects of novel therapeutics. Therefore, the present study assesses the quantification of inflammatory lung changes using positron emission tomography/magnetic resonance imaging (PET/MRI) of the lung in children and adolescents with CF and evaluates the possible impact of PET/MRI on individualized therapy management.

Methods: This monocentric, retrospective cohort study included 19 PET/MRI of the lung performed between 2014 and 2021 in 11 patients (16±4.5 years, 8–22 years; 7 females). PET acquisition was performed at least 20 minutes after i.v. application of a weight-adjusted dose of fluor-18-fluorodeoxyglucose (^{18}F-FDG) of 1 MBq/kgBW (mean effective dose, 1.3±0.4 mSv). Lesions of increased uptake were quantified based on standardized uptake values (SUV) and compared to background activity, liver and blood pool. Pulmonary changes were assessed using the established magnetic resonance imaging-CF (MR-CF) score and correlated to inflammatory lesions. Results were correlated to changes in therapy (initiation, modification or discontinuation of therapy after baseline-PET/MRI) based on the electronic medical records.

Results: Uptake was highly increased in 5 cases, moderate in 4 cases, low in 7 cases, no uptake in 3 cases. Most MR-CF score points were assigned to peribronchitis (23%) and air trapping (23%). Metabolically increased lesions were mainly interpreted as consolidations (59%; P<0.001) and mucus plugging (19%, P=0.024). There was a decrease in mean number and volumes of inflammatory lesions (P=0.016 each) and MR-CF score (P=0.047) between baseline and follow-up. After PET/MRI, therapy changed in 18 cases (95%; new medication: 58%, n=11; termination of therapy: 16%, n=3; modification of therapy: 21%, n=4).

Conclusions: In selected cases, pulmonary FDG-PET/MRI can help guide therapeutic decision-making and provide complementary information on CF-related lung changes to conventional MRI at a low radiation exposure.

^ ORCID: 0000-0002-4010-3034.

Keywords: Pulmonary cystic fibrosis (pulmonary CF); positron emission tomography (PET); magnetic resonance imaging (MRI); hybrid imaging; pediatrics

Submitted May 29, 2024. Accepted for publication Oct 31, 2024. Published online Dec 30, 2024.
doi: 10.21037/qims-24-989
View this article at: https://dx.doi.org/10.21037/qims-24-989

Introduction

Cystic fibrosis (CF) is the most common life-limiting autosomal recessive disorder in Europe (1). Despite improvements in diagnosis and therapy, lung disease remains the main cause of morbidity and mortality. Clinical severity and progression of CF over time are significantly influenced by the occurrence of lung infections (2). Highly sensitive and specific diagnostic tools are needed to help prevent chronic airway disease and enable early, personalized therapy. Clinical symptoms, pulmonary function tests, bronchial lavage or laboratory results are either non-specific (or non-sensitive) or invasive and therefore not convenient in the detection of early pulmonary changes or to monitor treatment effects (3-6).

Lung imaging plays an essential role in the diagnostic work-up of CF patient with chest computed tomography (CT) being the gold standard (5). Several studies have demonstrated the superiority of chest CT over other biomarkers in detecting acute and chronic airway changes (5,7). During the last decade, chest magnetic resonance imaging (MRI) has been established as feasible and sensitive alternative to CT without radiation exposure (8,9). Scoring systems have been established for various imaging techniques to enable quantification of treatment effect and disease progression (10,11). These include different morphologic lung changes like bronchiectasis, bronchial wall thickening, consolidation, mucus plugging or air trapping (8,12).

Previous developments in lung imaging now open up new possibilities for using MRI to assess structural and functional disorders in CF of the lung. Widespread repeated lung MRI allows not only for assessing disease progression but also for monitoring treatment response (13). Since the introduction of highly effective cystic fibrosis transmembrane conductance regulator (CFTR) modulator therapies, MRI can also assist in the evaluation of longitudinal effects of such novel therapeutics (14,15).

Despite the mentioned innovations, the differentiation of structural and inflammatory changes can be challenging: A consolidation can be caused by either atelectasis or inflammation but therapy might differ. ^{18}F-fluorodeoxyglucose (FDG)-positron emission tomography (PET) imaging could help with this problem as increased glucose metabolism is known to represent focal inflammation/infection (16,17). The few studies published on PET/CT in CF patients have demonstrated that a quantification of inflammation is possible with FDG-PET-imaging (18,19). Standalone MRI as a radiation free alternative has already been validated (10,20,21). To the best of our knowledge, PET/MRI, the combination of both techniques, has not been assessed in the context of pulmonary CF yet.

Therefore, this study aims to assess the quantification of inflammatory lung changes using PET/MRI of the lung in children and adolescents with CF and to evaluate the possible impact of PET/MRI on individualized therapy management. We present this article in accordance with the STROBE reporting checklist (available at https://qims.amegroups.com/article/view/10.21037/qims-24-989/rc).

Methods

The study was conducted in accordance with the Declaration of Helsinki (as revised in 2013). The study was approved by the Institutional Ethics Committee at the Medical Faculty of the Eberhard Karls University and at the University Hospital of Tübingen (No. 537/2021BO2) and individual consent for this retrospective analysis was waived. All patients or legal guardians gave signed consent for the clinically indicated PET/MRI. Separate informed consent for the study participation was waived. All study procedures were conducted in accordance with the Guidelines for Good Clinical Practice.

Study cohort

Between September 2014 and June 2021 19 FDG-PET/MRI examinations of 11 CF patients were included in this retrospective study (17 PET/MRI limited to the chest/

Table 1 Clinical data and PET/MRI findings for all included examinations

Exam No.	BL/FU	Effective dose (mSv)	MR-CF score	Lesions with increased FDG-uptake		Mean SUV_{peak}	Mean Uptake Score	Mean inflammatory index (ml$_l$)	FEV1 (%)	Vital capacity (%)	Therapy
				N	Volume (mL)						
1	BL	1.2	45	4	6	0.78	4.0	18	27	6	New medication
2	BL	2.3	44	22	190	2.61	3.5	684	32	38	New medication
3	FU	0.8	54	13	172	2.29	4.0	762	27	3	New medication
4	BL	0.7	24	17	54	1.23	4.1	215	75	74	New medication
5	FU	0.9	23	5	11	0.89	3.3	31	75	6	Therapy modified
6	FU	0.9	20	8	28	0.93	3.0	85	74	81	Therapy modified
7	BL	1.8	16	3	29	1.38	2.0	110	85	85	No change
8	BL	2.2	31	11	42	1.10	3.0	109	42	62	New medication
9	BL	1.4	30	27	86	2.40	4.1	357	39	7	New medication
10	FU	1.3	16	0	0	0	1.0	0	63	89	Therapy modified
11	BL	1.4	27	5	33	1.18	2.5	81	101	105	New medication
12	FU	1.2	19	8	35	1.27	2.0	83	6	77	Stop of medication
13	BL	1.6	25	5	94	0.93	2.3	275	86	93	New medication
14	FU	1.2	8	0	0	0	1.0	0	98	9	Stop of medication
15	BL	1.6	8	1	81	1.63	4.0	322	114	11	Stop of medication
16	BL	1.0	34	6	10	1.19	2.0	24	81	86	New medication
17	FU	1.0	20	0	0	0	1.0	0	N/A	N/A	Therapy modified
18	BL	1.0	32	8	15	0.81	2.2	37	56	71	New medication
19	BL	1.3	24	11	50	1.56	2.6	162	42	62	New medication

PET/MRI, positron emission tomography/magnetic resonance imaging; BL, baseline; FU, follow-up; MR-CF, magnetic resonance imaging-cystic fibrosis; FDG, fluorodeoxyglucose; SUV, standardized uptake value; FEV1, forced expiratory volume in one second; N/A, not available.

lungs and 2 whole-body PET/MRI). Seven patients were included with a baseline- and follow-up scan, including one patient with two follow-up scans (*Table 1*). All PET/MRI examinations were clinically indicated by the fact that physical examination, pulmonary function tests, laboratory results and prior non-contrast imaging (chest CT or MRI) were incohesive with regards to further treatment management. Children and adolescents with a prior diagnosis of CF (sweat test or gene sequencing) were eligible for the study if they were able to tolerate a fasting period of at least six hours over night before the PET/MRI. Exclusion criteria for PET/MRI were the need for supplemental oxygen, diabetes, pregnancy or metallic implants incompatible with MRI. The body mass index (BMI) was calculated for all patients as part of the PET/MRI planning.

Imaging protocol

The examination procedure of chest only PET/MRI is shown in *Figure 1*. All examinations were performed on a 3 Tesla PET/MRI scanner (Biograph mMR, Siemens Healthineers, Erlangen, Germany, software versions B20P and E11P) after a fasting period of at least 6 hours. Patients were positioned in supine position using a 32-channel-body array coil with respiratory gating belt.

^{18}F-FDG was administered intravenously at a target dose of 1.0 MBq/kgBW for PET/MRI of the chest and 2.0 MBq/kgBW for whole-body PET/MRI. Following the International Commission on Radiological Protection

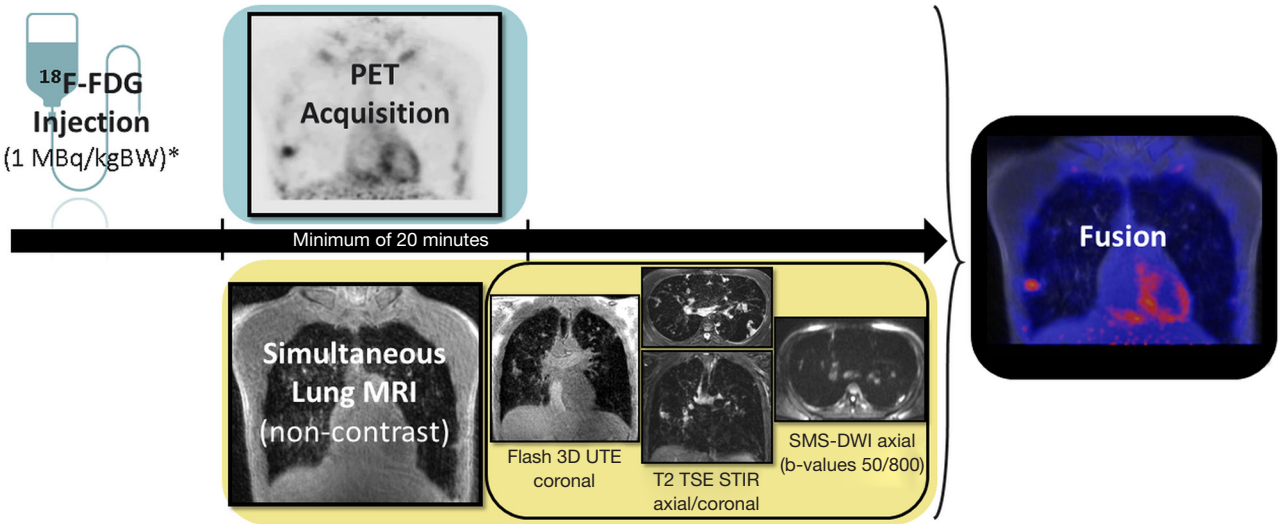

Figure 1 Examination procedure of hybrid PET/MRI. After intravenous administration of 18F-FDG at a target dose of 1.0 MBq/kgBW for chest-only PET/MRI (*2.0 MBq/kgBW if the PET was performed as part of a whole-body examination), PET acquisition was increased to a minimum of 20 minutes. Simultaneously, a non-contrast MRI of the lungs included the described diagnostic sequences. Color-coded fusion images were generated for the subsequent reading, which were used for the various quantification methods. FDG, fluorodeoxyglucose; PET, positron emission tomography; MRI, magnetic resonance imaging; UTE, ultrashort echo time; TSE, turbo spin echo; STIR, short-tau inversion recovery; SMS-DWI, simultaneous-multi-slice-accelerated diffusion-weighted imaging.

(ICRP) the effective dose was calculated as follows: The exactly measured administered dose of FDG (MBq) for each patient was multiplied by the suggested effective dose (mSv/MBq) of the corresponding age group (<1 year; 1–4 years; 5–9 years; 10–14 years; ≥15 years) (20). PET acquisition (and simultaneous MRI) started between 54–65 minutes after FDG administration, except one case with an uptake time of 128 minutes (mean, 64 minutes). The acquisition time was six minutes per bed position for whole-body PET/MRI, which includes one bed position for the lung in our standardized protocol. The acquisition time was increased to a minimum of 20 minutes for the chest-only PET/MRI (additional time depending on the number of sequences for the simultaneously acquired MRI) in order to obtain an adequate signal despite the low administered dose of FDG. PET imaging data were reconstructed applying an iterative Ordered Subset Expectation Maximization (OSEM) algorithm (matrix size, 256×256) with a 4 mm gaussian filter. Attenuation correction of emission data was performed using an MRI-based μ-map (5-compartment model including air, fat, water, tissue and bone) and syngo MR E11®/NUMARIS/4 (Siemens Healthineers) software.

A full diagnostic pulmonary MRI protocol for clinical routine use was applied in all study participants including coronal and transverse half-fourier acquisition single-shot turbo spin echo (HASTE) sequences, a coronal Flash 3D ultrashort echo time (UTE) spiral volume-interpolated breath-hold examination (VIBE) sequence, a coronal respiration-triggered T2w turbo-spin echo (TSE) sequence with short-tau inversion recovery (STIR) fat suppression and transversal simultaneous-multi-slice-accelerated diffusion weighted imaging (SMS-DWI) obtained at b-values of 50 and 800 s/mm^2 and including apparent diffusion coefficient (ADC) mapping. Detailed MRI scan parameters are given in *Table 2*. No contrast agent was used.

Image analysis

PET/MRI scans were analysed in clinical routine by a radiologist supervised by a speciality trained and certified pediatric radiologist (J.F.S., expert in pediatric radiology and chest imaging with over 25 years of experience) and a nuclear medicine physician (H.D., an expert in nuclear medicine with over 10 years of experience). One radiologist (R.S. with 5 years of experience in medical imaging) was blinded to all clinical data and the clinical radiology reports

Table 2 Summary of MRI acquisition parameters

Sequence	Orientation	TR (ms)	TE (ms)	Flip angle	Matrix size	Pixel spacing (mm)	Slice thickness (mm)	Additional information
HASTE	Coronal	1,200	91	120°	320×320	1.25×1.25	5	Free breathing
	Transversal		96	160°	256×154[†]	0.85×0.85		
Flash 3D UTE spiral VIBE	Coronal (transversal reconstruction)	2.84	0.05	5°	320×320	1.5×1.5	1.5	Breath hold, acquisition time 12–15 sec
T2w TSE with STIR	Coronal	4,000–7,000	60	150°–167°	256×160	1.75×1.75	5	Respiration-triggering
SMS-accelerated DWI	Transversal	2,500	52	90°	184×256	1.5×1.5	5	b-values 50 and 800 s/mm^2

[†], different matrix size in single cases. MRI, magnetic resonance imaging; TR, repetition time; TE, echo time; HASTE, half-fourier acquisition single-shot turbo spin echo; UTE, ultrashort echo time; VIBE, volume-interpolated breath-hold examination; TSE, turbo-spin echo; STIR, short-tau inversion recovery; SMS, simultaneous-multi-slice; DWI, diffusion-weighted imaging.

of the PET/MRI and assessed all exams additionally in the study setting. The visual assessment of focally increased FDG-uptake in the lung and correlation with morphology was analysed in a consensus reading by R.S. and M.E. (7 years of experience in medical imaging and certified pediatric radiology subspecialty). Image analysis was performed using the software syngo.via (version 9.4; Siemens Healthineers). All readers were offered a general training for syngo.via from the manufacturer. A training specifically aimed at the analysis of PET/MRI of the lungs did not take place. For the analyses presented below, a workflow optimized by the manufacturer for hybrid imaging was used. This included multiplanar reconstructions of the PET acquisition and the UTE sequence (uniplanar for the other MRI sequences), an automatic color-coded overlay and a maximum intensity projection (MIP) image of the PET data (*Figure 2*). It should be noted that although DWI sequences were included in the protocol, no separate ADC values of focal lesions were measured or correlations of ADC values were performed. The lungs were separated into the following six zones: right upper lobe (RUL), middle lobe (ML), right lower lobe (RLL), left upper lobe (LUL), lingula segment (LS), and left lower lobe (LLL).

Quantification of inflammation

A pulmonary lesion was defined as an area with higher uptake compared to the background activity. Semi-quantitative analysis was performed using conventional standard uptake values (SUV). Lesions were selected visually and measured with the volume of interest (VOI) isocontour segmentation tool using a threshold algorithm with a standard threshold of 40% of local VOI maximum (*Figure 2*). The mediastinal and hilar regions were excluded. The VOI isocontour shape formed a bounding area and the isocontour was created within that boundary. The total number of all lesions, lesion volumes and the 1-mL sphere at the region of highest uptake/pixel (SUV_{peak}) of every single lesion were measured automatically in each lung zone.

To evaluate the SUV independently of the exact applied FDG amount, individual patient characteristics (weight, height, BMI), and the uptake time values were referenced to the blood pool and liver uptake. An Uptake Score was calculated according to the established Deauville Score in lymphoma (21,22) with the average SUV (SUV_{mean}) of blood and liver compared to the SUV_{peak} of each lesion with increased FDG-uptake. The software automatically displayed a reference region for the blood pool as a cylinder with a height of 2 cm and a diameter of 1 cm, which was manually positioned in the left atrium. The automatically displayed liver reference region had a size of 3 cm in diameter, which was, if necessary, manually corrected to a position in the right lobe of the liver. The Uptake Score ranged from 1 to 5 as follows: 1, no uptake; 2, low uptake less or equal to the blood pool; 3, moderate uptake greater than the blood pool but less than the liver; 4, high uptake greater than the liver and 5, marked increased uptake, more than twice as much as the liver. Inflammation levels were classified as high with an Uptake Score of ≥4, moderate with an Uptake Score of 3 and low with an Uptake Score of 2.

A metabolic inflammatory index (ml_i) was calculated to consider volume and uptake intensity of inflammatory areas (n, number of inflammatory area) as follows: the products of inflammatory volume (Vol) and Uptake Score (US)

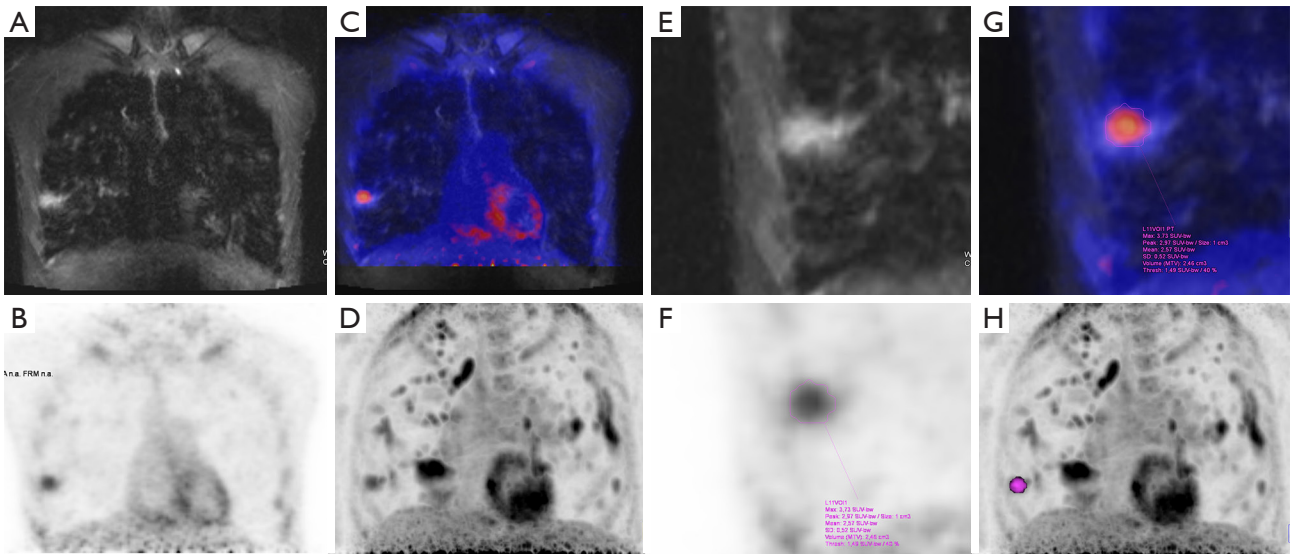

Figure 2 Exemplary presentation of the sequences and reconstructions used for lesion detection and quantification. A 22-year-old patient with CF. One consolidation in the middle lobe (A) which showed a markedly increased FDG-uptake (B-D, left side). Subsequent measurement of the lesion for quantification in the enlarged sections (E-H, right side). Coronal T2 TSE STIR (A), coronal reconstruction of corresponding PET slice (B), corresponding color-coded fusion image for lesion detection (C) and MIP image of PET (D) with focus on the lesion mentioned above. Enlarged section of coronal T2 TSE STIR (E), corresponding coronal image of PET slice with measurement of the lesion by isocontour segmentation of VOI (F), corresponding enlarged section of color-coded fusion image including the same measurement (G), MIP image of PET with colored marking of the measured lesion (H). CF, cystic fibrosis; FDG, fluorodeoxyglucose; TSE, turbo spin echo; STIR, short-tau inversion recovery; PET, positron emission tomography; MIP, maximum intensity projection; VOI, volume of interest.

of all lesions (and subdivided according to the different morphologic correlate) in each patient were summed up: $mI_i = \sum_{n=0-x} (Vol_n * US_n)$.

Correlation of morphologic parameters

Morphologic changes were analysed for the semi-quantitative magnetic resonance imaging-cystic fibrosis (MR-CF) score, which ranges from 0 to 72 (with 0 being the best and 72 points the worst). Primarily, coronary UTE sequence and axial reconstruction were used for this purpose, with the other conventional MRI sequences being used secondarily (in case of uncertainties or artifacts). As published previously the MR-CF score contains the following categories: bronchiectasis/bronchial wall thickening, mucus plugging, centrilobular opacities, sacculations, consolidations and air trapping (10). The MR-CF scores were determined separately by the reader R.S. as part of the study reading. Thereafter, visually selected areas of increased FDG-uptake (as described above) were correlated to the morphologic changes within consensus reading.

Changes in therapy

The electronic in-house medical records of all patients were subsequently analyzed using the software SAP NetWeaver (SAP, Walldorf, Germany) in order to assess possible therapy changes due to the current imaging results. Whether there was a possible effect on therapy was evaluated depending on the PET/MRI examination result (*Figure 3*). In the case of a positive test result or a worsening of inflammation, changes in therapy (application of a new drug, modification of the drug dose, discontinuation of therapy) were considered to influence the therapy regimen. If, on the other hand, the therapy was continued without changes or no new therapy was started, the positive examination findings had no influence on the choice of therapy. In the case of a negative examination result or improvement of lung findings, dose reduction and the continuation of an initiated therapy were

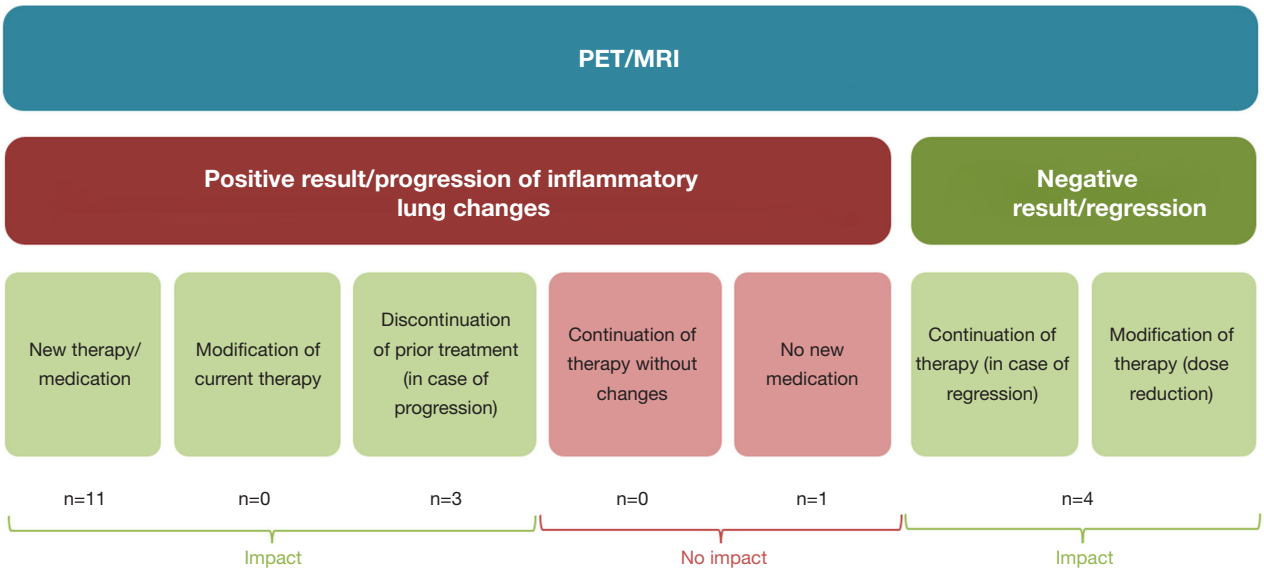

Figure 3 Changes of therapy management. Classification of all PET/MRI examinations into those with positive findings in terms of inflammatory lung changes or progression and negative findings or regression of previously known changes. Depending on this, different changes in the treatment regimen (if any) were evaluated as an influence of PET/MRI or no impact of PET/MRI. PET/MRI, positron emission tomography/magnetic resonance imaging.

evaluated as influence of the PET/MRI.

In addition, the results of other examinations were also extracted from the electronic medical records: All patients underwent pulmonary function tests using spirometry (Masterlab-Body; Jaeger, Würzburg, Germany) to assess global functional parameters such as forced expiratory volume in one second (FEV_1) and vital capacity (VC) within one week before/after PET/MRI examination (*Table 1*). Quantification of inflammatory, morphologic changes and pulmonary function tests were therefore compared between baseline and follow-up.

Statistical analysis

For statistical analysis SigmaStat, Version 27 via IBM SPSS Statistics (Armonk, NY, USA) was used. Descriptive statistics were used to characterize the study population. Shapiro-Wilk-Test was used to test for normal distribution.

The Spearman's rank-order correlation (Spearman correlation coefficient r_s) was used to compare SUVs of inflammatory volume with the MR-CF score and morphologic changes as well as pulmonary function tests. The correlation between treatment changes (according to *Figure 3*) and metric data (number of FDG positive lesions, MR-CF score) was calculated with the eta correlation coefficient (r_η). A correlation coefficient $r<0.1$ was interpreted as no correlation, $0.1\leq r\leq 0.3$ as weak, $0.3<r\leq 0.7$ as moderate and $r>0.7$ as strong. To assess the significance of the eta correlation coefficient, an analysis of variance (ANOVA) was first performed to determine if the means of the continuous variable differ significantly across the levels of the categorical variable. An F-statistic was then used to determine the corresponding P value. A low P value suggested that the relationship between the categorical variable and the continuous variable is unlikely to have occurred by chance.

For the evaluation of treatment effects, only patients with follow-up investigations were included (n=7). Primary and follow-up investigations were compared by using the non-parametric paired Wilcoxon-test. The effect size was computed with Cohen's d, considering $d\leq 0.2$ as low, $d\leq 0.5$ as moderate and $d\geq 1.1$ as high (23).

A receiver operating characteristic (ROC) analysis was performed to define cut-of levels in MR-CF score and number of FDG-positive lesions for changes in management. The cut-off values were selected by choosing the point of the ROC curve with the minimal distance to the left upper corner, thus optimising sensitivity and

Table 3 Distribution of inflammation and morphologic changes in the lung regions

Parameter	Right upper lobe	Middle lobe	Right lower lobe	Left upper lobe	Lingula segment	Left lower lobe
FDG + lesions in all patients (N)	47	23	25	23	10	26
Total inflammatory volume (mL)	201	322	120	87	111	89
Uptake Score [1–5]	3.1	3.4	2.9	3.2	3.9	3.1
MR-CF score	117	79	93	85	58	68

FDG, fluorodeoxyglucose; MR-CF, magnetic resonance imaging-cystic fibrosis.

specificity with equal weights. The area under the curve (AUC) was calculated for each ROC curve.

All statistical tests were considered significant when $P<0.05$.

Results

Patient characteristics

Nineteen FDG PET/MRI studies of 11 patients between the age of 8–22 years (mean ± standard deviation, 16±4.5 years; 7 females, 4 males) were included. Indication for PET/MRI were the following: unexpected worsening of lung function (n=5), prolonged signs of infection despite intensive therapy (n=4), exclusion of severe inflammatory focus before liver transplantation (n=3) and response assessment/follow-up after baseline PET/MRI (n=7). The mean time between baseline and follow-up PET/MRI was 4±2 months. Mean BMI was 18.8±2.4 kg/m^2. The majority of patients (6/11) had received a native MRI of the thorax within three months before the baseline PET/MRI, a further two patients at a greater time interval before the PET/MRI (more than 7 months). One patient had an X-ray and one a CT of the thorax as a preliminary examination. One patient did not receive prior imaging at our clinic.

PET/MRI parameters

The mean effective dose was 1.3±0.4 mSv. Effective dose for each examination is given in *Table 1*. The average total scanning time for PET/MRI of the lung (one bed position) was 20.8±5.7 minutes (range, 6 to 30 minutes).

Quantification of inflammation

PET/MRI showed a total number of 154 areas with increased FDG-uptake compared to the background with an average of 8±7 areas per patient (range, 0–27 areas). The mean inflammatory volume per patient was 58±14 mL (range, 0–190 mL). Most of the areas were in the RUL (n=47), least in the LS (n=10) and otherwise equally distributed in the other lung zones (*Table 3*). The distribution of the inflammatory volume showed an accentuation of the ML and the RUL. When comparing each side separately, the middle lung zones (ML and LS) had the largest volumes.

PET/MRI showed 5 examinations with a high (Uptake Score of ≥4), 4 with a moderate (Uptake Score of 3) and 7 with a low mean (Uptake Score of 2) inflammation level. Three examinations did not show areas of an increased FDG-uptake (Uptake Score of 1). Uptake Scores for each examination are given in *Table 1*. The mean overall inflammatory index of all patients was 176.7±221.6 ml_i (range, 0–762 ml_i).

Analysis and correlation of morphologic parameters

The mean MR-CF score of all included patients was 26±12 (range 8 to 54). Most points of the MR-CF score were given in the upper lung lobes, followed by the lower lobes, least in the middle lung zones (*Table 3*). Most points of the MR-CF score were given due to bronchial wall thickening (23%) and air trapping (23%), followed by mucus plugging (18%), centrilobular opacities (18%), consolidations (13%) and sacculations (8%). MR-CF scores for each scan are given in *Table 1*.

Areas with increased FDG-uptake (inflammatory changes according to the inflammatory index) were interpreted most often as consolidations (59%, Spearman correlation coefficient $r_s=0.759$, $P<0.001$) followed by mucus plugging (19%, $r_s=0.514$, $P=0.024$), bronchial wall thickening (9%), centrilobular opacities (8%), sacculations (5%). Consolidations accounted for the largest proportion (53%) of total inflammatory volume.

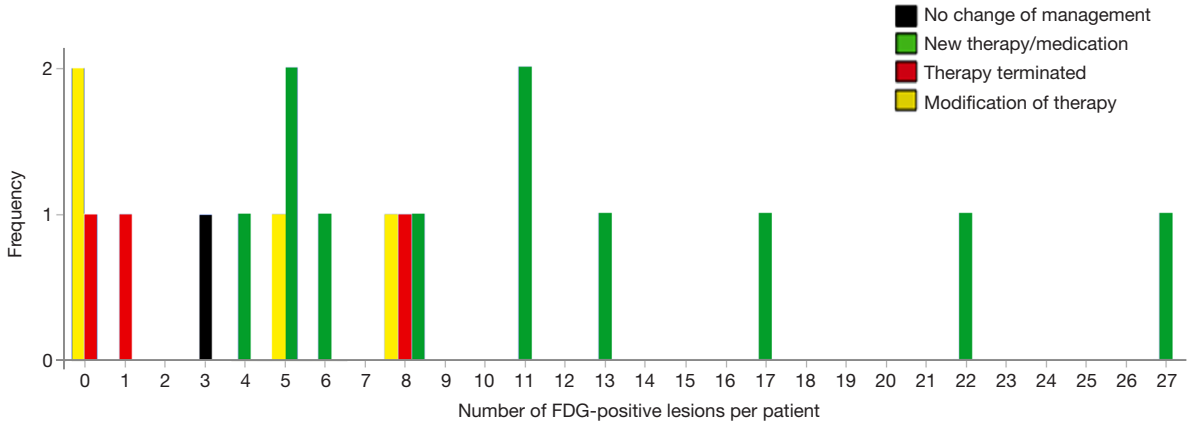

Figure 4 Number of inflammatory lesions and following therapeutic procedure. Number of inflammatory lesions per patient with respective frequency and color coded bars with regard to therapeutic consequence. FDG, fluorodeoxyglucose.

Changes in therapy

After the PET/MRI, therapy was altered in 18/19 cases (95%): in examinations with a positive result or increase in inflammatory changes, a new medication/therapy was started in 11 cases (58%), a previously started antibiotic therapy was terminated (in case of progression) in 3 cases (16%) and CFTR modulator therapy was continued without any changes in one patient (5%). The cases in which a new therapy was started concerned the start of a CFTR modulator therapy (elexacaftor/tezacaftor/ivacaftor, Kaftrio®/Trikafta®; n=5), application of new antibiotics (combination of ceftazidime and tobramycin; n=3), initiation of an (additional) systemic antimycotic therapy (n=2), a new inhalation therapy [nitric oxide (NO) or tiotropium; n=2] and a systemic steroid therapy as a high dose intravenous pulse therapy (methylprednisolone; n=2). In 4 cases with a negative results or improved findings, continued therapy was modified in 4 cases in terms of dose reduction (21%; *Table 1*; *Figure 3*). In all of these cases, the dose of a CFTR modulator was adjusted.

There was a moderate positive correlation between treatment changes (according to *Figure 3*) and the number of FDG positive lesions (rη=0.587 P=0.034) as well as treatment changes and the MR-CF score (rη=0.760 P=0.001): A small number of FDG positive lesions and/or a low MR-CF-Score correlated to a dose reduction or termination of therapy, a high number of inflammatory lesions and a high MR-CF score correlated with the start of a new medication. The ROC-analysis determined cut-off values associated with the initiation of a new therapy for more than 3 inflammatory areas (AUC 0.875, sensitivity 100%, specificity 63.5%, P<0.01; *Figure 4*) or a MR-CF score of more than 23 points (AUC 1.0, sensitivity 100%, specificity 100%, P<0.001; *Figure 5*).

Monitoring therapeutic effects in follow-up studies

The mean number and mean volume of all inflammatory lesions decreased between baseline (13±9 areas; 73±60 mL) and follow-up (4±5 areas; 43±64 mL; P=0.016 both, r=0.63 both; *Figure 6*). In addition, there was a marked difference concerning the inflammatory index between baseline (249±224) and follow-up (171±285; P=0.297). The decline in the mean Uptake Score was also not significant (P=0.156).

The MR-CF score showed a significant decrease between baseline and follow-up (baseline 31±7, follow-up 21±16; P=0.047; *Figure 6*). Considering the subcategories, there was a significant change for bronchial wall thickening (mean points baseline 7.0±2.7 and follow-up 4.6±3.1, P=0.031), but not for the other morphological features.

Considering the morphological correlates, there was a significant decrease of the inflammatory volume and inflammatory index between baseline and follow-up concerning mucus plugging (volume: 19±16 to 3±4 mL; P=0.016; r=0.63; inflammatory index: 68.8±64 to 8.6±13.9 ml_i; P=0.016; r=0.63). Marked changes of centrilobular opacities were not statistically significant (volume: 13±10 to 0.9±2 mL; P=0.043; inflammatory index: 36±33 to 1.8±3.8 ml_i; P=0.063; r=0.63). No significant changes were also seen for bronchial wall thickening, consolidation and air trapping.

There was a moderate negative correlation between FEV1 and the number of FDG positive lesions (r_s=–0.613,

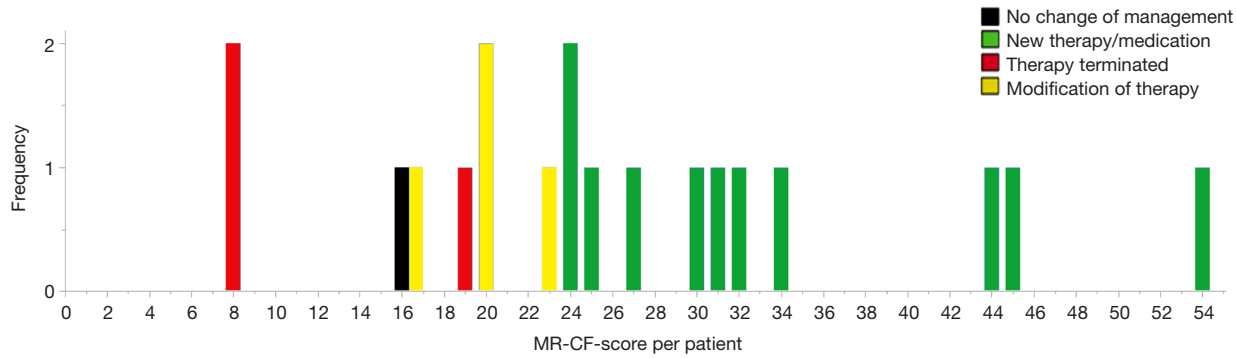

Figure 5 MR-CF score and following therapeutic procedure. MR-CF score per patient with respective frequency and color coded bars with regard to therapeutic consequence. A ROC analysis with maximized sensitivity and specificity showed a cut-off value of >23 points for starting a new medication. MR-CF, magnetic resonance imaging-cystic fibrosis; ROC, receiver operating characteristic.

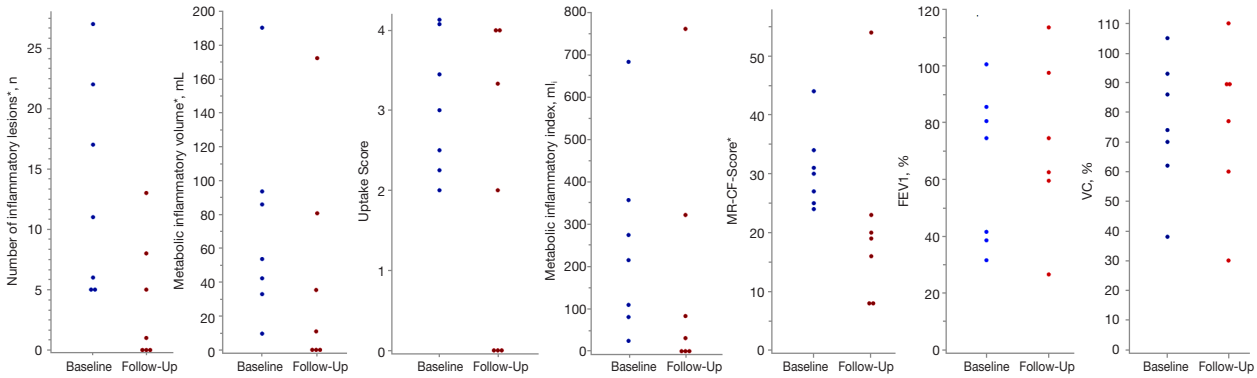

Figure 6 Differences between baseline and follow up. Development of different quantitative morphological and functional parameters starting from baseline and in follow-up examination shown as single data points of each patient (n=7). *, significant at the level P<0.05. MR-CF, magnetic resonance imaging-cystic fibrosis; FEV1, forced expiratory volume in one second; VC, vital capacity.

P=0.007) as well as FEV1 and MR-CF score (r_s=−0.658, P=0.003). Pulmonary function tests themselves showed no significant differences between baseline (FEV1 65%±27%, VC 75%±22%) and follow-up (FEV1 73%±30%, VC 76%±27%; *Figure 6*). There was no correlation with the inflammatory index or the therapeutic regime.

Discussion

This is the first study investigating the role of PET/MRI in children and adolescents with pulmonary CF. This hybrid approach provides a variety of quantitative data concerning inflammatory lung changes, some of which correlate to morphological features. In our cohort, the findings led to changes in subsequent treatment decisions. Equally, PET/MRI seems appropriate for the depiction of treatment effects during therapy in addition to assessment of chronic structural lung changes. PET/MRI bears a low radiation dose, also compared to PET/CT (18,19), but similar to low-dose CT (24,25).

In accordance to PET/CT studies (18,19), our results show that PET/MRI can be used to quantify inflammation in CF patients with lung disease. Localized foci of increased FDG uptake are characteristic for focal inflammation as described by Chen *et al.* (26), Klein *et al.* (18) and Amin *et al.* (19) (*Figure 2*). Other study groups compared the background enhancement of the lung in CF patients with or without acute exacerbation to control subjects: Klein *et al.* (18) demonstrated that background lung activity was higher in acute inflammations, whereas Chen *et al.* (27)

Table 4 PET/MRI findings of all included patients according to different morphologic correlates

Categories of MR-CF score	Lesions with increased FDG-uptake		SUVpeak (mean ± SD)	Uptake Score (mean ± SD)	Inflammatory index (mean ml_i ± SD)
	N	Volume (mL)			
Bronchial wall thickening	16	108	1.19±0.58	2.6±1.0	16±34
Mucus plugging	65	184	1.36±0.61	3.2±0.9	33±48
Centrilobular opacities	18	101	1.08±0.37	3.2±0.9	15±26
Consolidation	44	495	2.53±2.97	3.8±0.9	104±178
Sacculation	10	45	1.88±1.16	3.1±1.2	8±22
Air trapping	0	0	0±0	0±0	0±0

PET/MRI, positron emission tomography/magnetic resonance imaging; MR-CF, magnetic resonance imaging-cystic fibrosis; FDG, fluorodeoxyglucose; SUV, standardized uptake value; SD, standard deviation.

found even lower whole lung SUV in CF patients compared to healthy controls. Due to this discrepancy, we focused on measuring the SUV of affected focal inflammation spots.

Amin *et al.* (19) showed SUV_{mean} reflecting diffuse inflammation which persists over time and SUV_{max} representing acute inflammation which is more beneficial for intervention adaptions. We decided to measure the SUV_{peak} to evaluate changes during therapy monitoring. SUV_{peak} is comparable to SUV_{max} but represents not only the voxel with the highest SUV in a focal inflammation spot but the SUV of the 1 mL area around this spot therefore might be more robust against outliers.

Inaccurate measuring of weight, tracer dose, fasting, acquisition time and extravasation or remaining tracer in the injection tube are known to possibly have a large effect on SUV measurements (21). In order to minimize those errors, the SUV_{peak} of the focal areas were compared to the SUV_{mean} of liver and blood pool for each patient. We included an approach of standardized reporting following the Deauville Score used in Hodgkin lymphoma (21) which was adjusted for the evaluation of inflammation levels in PET/MRI of the lung (Uptake Score; *Table 4*). Similar studies used empirical working thresholds bearing the risk of higher influence of the mentioned errors (18,27). Besides, Klein *et al.* (18) assumed that progressive tissue destruction and reduced blood supply to certain parts of the lung (due to lung changes in CF patients) result in lower FDG uptake. This could result in lower SUV of focal inflammatory activity despite infection and could be normalized by the use of the newly derived Uptake Score. The reproducibility of this score should be validated in further prospective approaches to allow a more frequent use in the future.

Our study is the first to measure the volume and the inflammatory index of pulmonary inflammatory changes as additional quantification parameters. Previous studies suggested that treatment response was deduced due to a decrease in numbers or SUV of focal increased metabolic activity (18,19,26,27). Our results show that the number, volume and SUV are not necessarily impacted in the same manner: consolidations had the highest percentage of total volume and also the highest portion of focal metabolic activity (*Table 4*). In concordance to other studies, our results show a treatment response in the mean number of FDG positive lesions regardless to morphologic correlates (*Figure 6*). However, for mucus plugging only the volume and the inflammatory index (considering volume and FDG-uptake) were statistically significant, whereas number and SUV showed no significant influence. This suggests, that adding the lesion volume and inflammatory index as additional quantification markers could maybe more clearly depict therapeutic changes, which are otherwise less evident when comparing numbers and SUV only.

Our data confirms that the semi-quantitative Tuebinger MR-CF score (10) is effective to estimate morphologic lung changes on the simultaneously acquired MR-images during PET/MRI. Although both, the inflammatory index and the MR-CF score revealed a good correlation to each other, they represent different aspects of disease and associated inflammatory changes. This observation is in line with results of other study groups: Amin *et al.* (19) concluded that PET is likely able to reveal early inflammatory changes, whereas CT helps to identify late structural changes related to chronic inflammation. Klein *et al.* (18) found further changes on CT imaging that were not seen on PET scans, but in contrast to CT findings PET helped to differentiate between acute and chronic changes. Chen

et al. (27) identified that similar morphologic changes of the lung may show corresponding FDG-uptake in some patients while other cases will be FDG negative. Similar to our study results, they found a non-uniform distribution of FDG-uptake within the lung zones and postulated that such regional measurements could be more sensitive in detecting anti-inflammatory effects of novel therapy than global measurements (26). As discussed in our previous study (10), the scores used so far, both in CT and MRI, refer to morphological parameters. The additional PET measurements could therefore not only help to recognize the inflammatory components, but also to better assess the significance of the morphological changes and quantify their severity. Air trapping as a functional parameter of the MR-CF score is given less consideration in the current study, as no focal uptake can be measured.

The presented data suggests that the inflammatory index (derived from PET measurements) reflects more consolidation and mucus plugging whereas the MR-CF score captures more the functional aspects such as air trapping and bronchial wall thickening. These findings partially agree with the observations of Klein *et al.* that did not show corresponding FDG uptake for the morphologic correlate of bronchial wall thickening and bronchiectasis (18). In contrast to our results, Amin *et al.* have not seen an FDG correlate to mucus plugging (19). These differences might be due to small cohorts with a maximum of 20 patients in all comparable studies (18,19,26). In addition, PET/MRI of the lung is not part of the routine workup of CF patients. Therefore, only patients with special clinical indications (mostly severe disease) were investigated with this method, which can result in selection bias.

With regard to therapy management, valuable information provided by PET/MRI may help in this particular patient population in the future. PET/MRI can assist with patient management if the current state of the disease remains unclear based on the clinical picture and previous conventional diagnostics. In our clinical setting, this new quantitative approach proved to be promising and was associated with therapeutic consequences (95% of all examinations, 18/19). The proposed cut-off levels for the MR-CF score and the number of inflammatory lesions serve only as approximate calculations in order to illustrate possible future applications and the feasibility in the context of the PET/MRI measurements. Prospective studies and randomized trials for validation would be necessary to evaluate implications for changes in management.

The following limitations need to be considered in this study: The main limitations are the retrospective study design and a small patient cohort, which makes statistic evaluation difficult and limits the generalizability of the results. A potential confounding factor is the selection of the patient collective, which is, however, an inherent limitation of the study, as the underlying disease is already rare, but the use of PET/MRI for this indication is also rare. The possible approach of using a (healthy) comparison group was not available for this evaluation. Indications for PET/MRI varied, only a part of the patients received a follow-up investigation (n=7) and the evaluation of treatment effects occurred under different therapeutic approaches. Changes due to novel therapy options could therefore have a greater impact in the study cohort than in a representative CF patient population. Another limitation is that the inter-observer variability was not measured for the FDG-PET measurements. Although DWI sequences were included in the protocol, no analysis of focal ADC values was performed. The value of DWI for structural lung changes has not been finally validated, so this method could be investigated separately with correlation of ADC values to SUV measurements (28).

Conclusions

We conclude that in selected cases pulmonary FDG-PET/MRI can help guide therapeutic decision-making and provide complementary information on CF-related lung changes to conventional MRI at a low radiation exposure. Further prospective studies are needed to confirm these findings and to select appropriate patient subgroups.

Acknowledgments

We thank the patients and clinical staff involved in this study. We thank Dr. Sergios Gatidis, MD (Stanford Department of Radiology, Stanford, CA, USA) for the valuable support with methodological aspects of the study. We also thank Julian Philipp Schwarz (Bosch Sensortec GmbH, Reutlingen, Germany) for his technical support with statistical analysis and assistance in intellectual discussions.
Funding: None.

Footnote

Reporting Checklist: The authors have completed the STROBE reporting checklist. Available at https://qims.amegroups.com/article/view/10.21037/qims-24-989/rc

Conflicts of Interest: All authors have completed the ICMJE uniform disclosure form (available at https://qims.amegroups.com/article/view/10.21037/qims-24-989/coif). The authors have no conflicts of interest to declare.

Ethical Statement: The authors are accountable for all aspects of the work in ensuring that questions related to the accuracy or integrity of any part of the work are appropriately investigated and resolved. The study was conducted in accordance with the Declaration of Helsinki (as revised in 2013). The study was approved by the Institutional Ethics Committee at the Medical Faculty of the Eberhard Karls University and at the University Hospital of Tübingen (No. 537/2021BO2) and individual consent for this retrospective analysis was waived. All patients or their legal guardians gave signed consent for the clinically indicated PET/MRI. Separate informed consent for the study participation was waived. All study procedures were conducted in accordance with the Guidelines for Good Clinical Practice.

References

1. Elborn JS. Cystic fibrosis. Lancet 2016;388:2519-31.
2. Cantin AM, Hartl D, Konstan MW, Chmiel JF. Inflammation in cystic fibrosis lung disease: Pathogenesis and therapy. J Cyst Fibros 2015;14:419-30.
3. Nixon GM, Armstrong DS, Carzino R, Carlin JB, Olinsky A, Robertson CF, Grimwood K, Wainwright C. Early airway infection, inflammation, and lung function in cystic fibrosis. Arch Dis Child 2002;87:306-11.
4. Dakin CJ, Numa AH, Wang H, Morton JR, Vertzyas CC, Henry RL. Inflammation, infection, and pulmonary function in infants and young children with cystic fibrosis. Am J Respir Crit Care Med 2002;165:904-10.
5. Tiddens HA, Rosenow T. What did we learn from two decades of chest computed tomography in cystic fibrosis? Pediatr Radiol 2014;44:1490-5.
6. Wainwright CE, Grimwood K, Carlin JB, Vidmar S, Cooper PJ, Francis PW, Byrnes CA, Whitehead BF, Martin AJ, Robertson IF, Cooper DM, Dakin CJ, Masters IB, Massie RJ, Robinson PJ, Ranganathan S, Armstrong DS, Patterson LK, Robertson CF. Safety of bronchoalveolar lavage in young children with cystic fibrosis. Pediatr Pulmonol 2008;43:965-72.
7. de Jong PA, Lindblad A, Rubin L, Hop WC, de Jongste JC, Brink M, Tiddens HA. Progression of lung disease on computed tomography and pulmonary function tests in children and adults with cystic fibrosis. Thorax 2006;61:80-5.
8. Eichinger M, Optazaite DE, Kopp-Schneider A, Hintze C, Biederer J, Niemann A, Mall MA, Wielpütz MO, Kauczor HU, Puderbach M. Morphologic and functional scoring of cystic fibrosis lung disease using MRI. Eur J Radiol 2012;81:1321-9.
9. Wielpütz MO, Puderbach M, Kopp-Schneider A, Stahl M, Fritzsching E, Sommerburg O, Ley S, Sumkauskaite M, Biederer J, Kauczor HU, Eichinger M, Mall MA. Magnetic resonance imaging detects changes in structure and perfusion, and response to therapy in early cystic fibrosis lung disease. Am J Respir Crit Care Med 2014;189:956-65.
10. Schaefer JF, Hector A, Schmidt K, Teufel M, Fleischer S, Graepler-Mainka U, Riethmueller J, Gatidis S, Schaefer S, Nikolaou K, Hartl D, Tsiflikas I. A semiquantitative MRI-Score can predict loss of lung function in patients with cystic fibrosis: Preliminary results. Eur Radiol 2018;28:74-84.
11. Breuer O, Caudri D, Stick S, Turkovic L. Predicting disease progression in cystic fibrosis. Expert Rev Respir Med 2018;12:905-17.
12. Szczesniak R, Turkovic L, Andrinopoulou ER, Tiddens HAWM. Chest imaging in cystic fibrosis studies: What counts, and can be counted? J Cyst Fibros 2017;16:175-85.
13. Dournes G, Walkup LL, Benlala I, Willmering MM, Macey J, Bui S, Laurent F, Woods JC. The Clinical Use of Lung MRI in Cystic Fibrosis: What, Now, How? Chest 2021;159:2205-17.
14. Graeber SY, Renz DM, Stahl M, Pallenberg ST, Sommerburg O, Naehrlich L, et al. Effects of Elexacaftor/Tezacaftor/Ivacaftor Therapy on Lung Clearance Index and Magnetic Resonance Imaging in Patients with Cystic Fibrosis and One or Two F508del Alleles. Am J Respir Crit Care Med 2022;206:311-20.
15. David M, Benlala I, Bui S, Benkert T, Berger P, Laurent F, Macey J, Dournes G. Longitudinal Evaluation of Bronchial Changes in Cystic Fibrosis Patients Undergoing

Elexacaftor/Tezacaftor/Ivacaftor Therapy Using Lung MRI With Ultrashort Echo-Times. J Magn Reson Imaging 2024;60:116-24.
16. Labiris NR, Nahmias C, Freitag AP, Thompson ML, Dolovich MB. Uptake of 18fluorodeoxyglucose in the cystic fibrosis lung: a measure of lung inflammation? Eur Respir J 2003;21:848-54.
17. Chen DL, Rosenbluth DB, Mintun MA, Schuster DP. FDG-PET imaging of pulmonary inflammation in healthy volunteers after airway instillation of endotoxin. J Appl Physiol (1985) 2006;100:1602-9.
18. Klein M, Cohen-Cymberknoh M, Armoni S, Shoseyov D, Chisin R, Orevi M, Freedman N, Kerem E. 18F-fluorodeoxyglucose-PET/CT imaging of lungs in patients with cystic fibrosis. Chest 2009;136:1220-8.
19. Amin R, Charron M, Grinblat L, Shammas A, Grasemann H, Graniel K, Ciet P, Tiddens H, Ratjen F. Cystic fibrosis: detecting changes in airway inflammation with FDG PET/CT. Radiology 2012;264:868-75.
20. ICRP. Radiation dose to patients from radiopharmaceuticals. Addendum 3 to ICRP Publication 53. ICRP Publication 106. Approved by the Commission in October 2007. Ann ICRP 2008;38:1-197.
21. Barrington SF, Qian W, Somer EJ, Franceschetto A, Bagni B, Brun E, Almquist H, Loft A, Højgaard L, Federico M, Gallamini A, Smith P, Johnson P, Radford J, O'Doherty MJ. Concordance between four European centres of PET reporting criteria designed for use in multicentre trials in Hodgkin lymphoma. Eur J Nucl Med Mol Imaging 2010;37:1824-33.
22. Meignan M, Gallamini A, Meignan M, Gallamini A, Haioun C. Report on the First International Workshop on Interim-PET-Scan in Lymphoma. Leuk Lymphoma 2009;50:1257-60.
23. Cohen J. A power primer. Psychol Bull 1992;112:155-9.
24. Esser M, Hess S, Teufel M, Kraus MS, Schneeweiß S, Gatidis S, Schaefer JF, Tsiflikas I. Radiation Dose Optimization in Pediatric Chest CT: Major Indicators of Dose Exposure in 1695 CT Scans over Seven Years. Rofo 2018;190:1131-40.
25. Tsiflikas I, Thomas C, Ketelsen D, Seitz G, Warmann S, Claussen CD, Schäfer JF. High-pitch computed tomography of the lung in pediatric patients: an intraindividual comparison of image quality and radiation dose to conventional 64-MDCT. Rofo 2014;186:585-90.
26. Chen DL, Ferkol TW, Mintun MA, Pittman JE, Rosenbluth DB, Schuster DP. Quantifying pulmonary inflammation in cystic fibrosis with positron emission tomography. Am J Respir Crit Care Med 2006;173:1363-9.
27. Chen DL, Atkinson JJ, Ferkol TW. FDG PET imaging in cystic fibrosis. Semin Nucl Med 2013;43:412-9.
28. Ciet P, Serra G, Andrinopoulou ER, Bertolo S, Ros M, Catalano C, Colagrande S, Tiddens HA, Morana G. Diffusion weighted imaging in cystic fibrosis disease: beyond morphological imaging. Eur Radiol 2016;26:3830-9.

Cite this article as: Schwarz R, Schäfer JF, Utz P, Graepler-Mainka U, Dittmann H, Kraus MS, Esser M. Application of low-dose FDG-PET/MRI for quantification of lung changes in pediatric patients with cystic fibrosis: a new inflammatory index. Quant Imaging Med Surg 2025;15(1):189-202. doi: 10.21037/qims-24-989

